Efficiency Limiting Factors in Perovskite Solar Cells

Hideo Ohkita and Hyung Do Kim

Kyoto University, Graduate School of Engineering
Katsura, Nishikyo, Kyoto 615-8510, Japan
Phone: +81-75-383-2612 Fax: +81-75-383-2617 E-mail: ohkita@photo.polym.kyoto-u.ac.jp

In this study, we have discussed how grain sizes of $CH_3NH_3PbI_3$ perovskites have an impact on the photovoltaic parameters such as a short-circuit current density J_{SC}, an open-circuit voltage V_{OC}, and hence a power conversion efficiency PCE. As a result, we found that the device with larger grains exhibits the better photovoltaic parameters. The highest PCE was as high as 19.4%, which was obtained for the device with a grain size of ~500 nm. We further discuss the efficiency limiting factors in terms of the grain size of $CH_3NH_3PbI_3$ in perovskite solar cells.

1. Introduction

Organic–inorganic hybrid metal-halide perovskite solar cells have attracted a great deal of attention in recent years, because they can be fabricated by solution processes even though they are inorganic semiconductors. Consequently, they have made extremely rapid progress in the last decade. The power conversion efficiency (PCE) has been drastically improved up to more than 20%[1–3] since the first report by Miyasaka and his co-workers was published in 2009.[4] In the early stage, on the other hand, there have been several issues to be solved such as poor reproducibility and large hysteresis in the current density–voltage (*J*–*V*) characteristics.[5–7] As such, it was virtually impossible to discuss the device physics or photovoltaic mechanisms in terms of the device parameters. Recent studies have shown that flat and pinhole-free perovskite layers can be fabricated with high reproducibility and less hysteresis by solvent engineering techniques.[8–10] In this study, we have fabricated flat and pinhole-free perovskite layers by the fast-deposition crystallization (FDC) method reported by Cheng and his coworkers.[9] On the basis of the *J*–*V* characteristics, we discuss the dependence of grain sizes in perovskite layer on the photovoltaic parameters.[11]

2. Experimental

Sample preparation

Methylammonium iodide (CH_3NH_3I) was prepared by adding a methanol solution of methylamine (CH_3NH_2) dropwisely to an aqueous solution of hydrogen iodide (HI) in a 500 mL round bottom flask at 0 °C. Methylammonium lead iodide ($CH_3NH_3PbI_3$) was prepared by mixing CH_3NH_3I with purified lead iodide (PbI_2) at a molar ratio of 1 to 1 in anhydrous *N*,*N*-dimethylformamide (DMF), and then stirred at 70 °C overnight in a nitrogen-filled glove box. The weight concentration of $CH_3NH_3PbI_3$ in the DMF solution was varied from 25, 45, and 55 wt% to give $CH_3NH_3PbI_3$ grains with different sizes in the following device fabrication.

Device fabrication

A dense TiO_2 layer was coated on an F-doped tin-oxide (FTO) substrate by spray-pyrolysis at 470 °C from an ethanol solution of bis(isopropoxide)bis(acetylacetonato)titanium(IV). On the basis of the fast-deposition crystallization (FDC) method reported previously,[9] a $CH_3NH_3PbI_3$ layer was prepared on the dense TiO_2 layer by spincoating from the three different DMF solutions of $CH_3NH_3PbI_3$. During the spincoating, anhydrous chlorobenzene was quickly dropped onto the center of the substrate, resulting in the instant color change in the $CH_3NH_3PbI_3$ layer from yellow to brown. The perovskite-coated substrate was dried at 100 °C for 10 min. Subsequently, a hole transporting-layer was prepared on the perovskite-coated substrate by spincoating from an anhydrous chlorobenzene solution of 2,2', 7,7'-tetrakis(*N*,*N*-di-*p*-methoxyphenylamine)-9,9-spirobifluorene (spiro-OMeTAD) with 4-*tert*-butylpyridine and lithium bis(trifluoromethanesulfonyl)imide. Finally, a gold layer was thermally deposited on top of the active layer under vacuum. The final layered device structure is as follows: FTO/dense-TiO_2/$CH_3NH_3PbI_3$/spiro-OMeTAD/Au.

Measurements

Current density–voltage (*J*–*V*) characteristics of the devices were measured under the AM1.5G simulated solar illumination with an intensity of 100 mW cm^{-2}. The light intensity was corrected with a calibrated silicon photodiode reference cell. The external quantum efficiency (EQE) spectra were obtained with a spectral response measurement system. All the devices were measured in a nitrogen atmosphere with a metal mask to give an

active area of 0.09 cm^2. The surface morphology and thickness of perovskite films were measured with an atomic force microscope (AFM) with a silicon probe in contact mode and a scanning electron microscope (SEM).

3. Results and Discussion

Film morphology

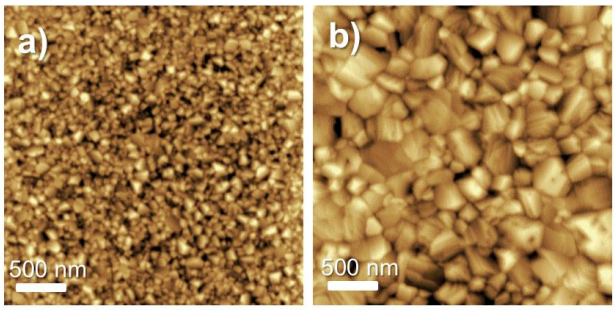

Fig. 1. AFM images of $CH_3NH_3PbI_3$ films fabricated by the FDC method from a DMF solution of $CH_3NH_3PbI_3$ with different weight concentrations: a) 25 wt% and b) 55 wt%. The scale bars correspond to 500 nm in length.

Figure 1 shows the AFM images of $CH_3NH_3PbI_3$ films fabricated by the FDC method. As shown in the figure, relatively flat and pinhole-free $CH_3NH_3PbI_3$ layers were obtained. The larger grains were found in $CH_3NH_3PbI_3$ films fabricated from the more concentrated solutions. Figure 2 shows the relationship between the film thickness L and grain size of the three different $CH_3NH_3PbI_3$ layers. As shown in the figure, the thickness was almost the same as the grain size although wider distribution in the grain size was found for the thicker films. This agreement suggests that $CH_3NH_3PbI_3$ layers consist of monograins in the direction normal to the substrate. Such monograin-like structures are also found in the cross-sectional SEM image of the $CH_3NH_3PbI_3$ layer with an average grain size of 500 nm as shown in Figure 3. This structure would be beneficial for charge transport to each electrode in the direction normal to the substrate.

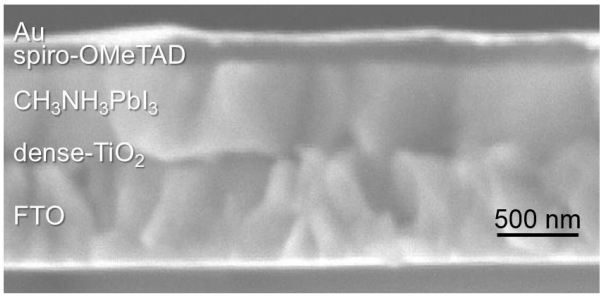

Fig. 3. A cross-sectional SEM image of a perovskite solar cell prepared from 55 wt% $CH_3NH_3PbI_3$ solution. The scale bar corresponds to 500 nm in length.

Photovoltaic performance

Figure 4 shows J–V characteristics of a perovskite solar cell prepared from 55 wt% $CH_3NH_3PbI_3$ solution. In the reverse scan, a short-circuit current density (J_{SC}) was 23.92 mA cm^{-2}, an open-circuit voltage (V_{OC}) was 1.08 V, a fill factor (FF) was 0.750, and a PCE was 19.4%. More importantly, as shown in the figure,

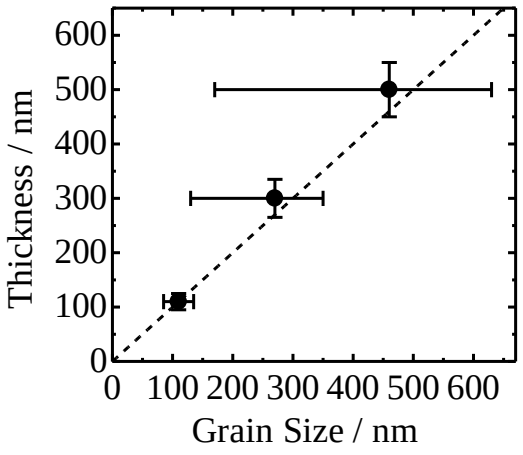

Fig. 2. Thickness of $CH_3NH_3PbI_3$ layers plotted against grain sizes. The closed circles and error bars represent the average and standard deviation analyzed for eight different AFM images of the $CH_3NH_3PbI_3$ films, respectively. The broken line represents a linear relationship between them.

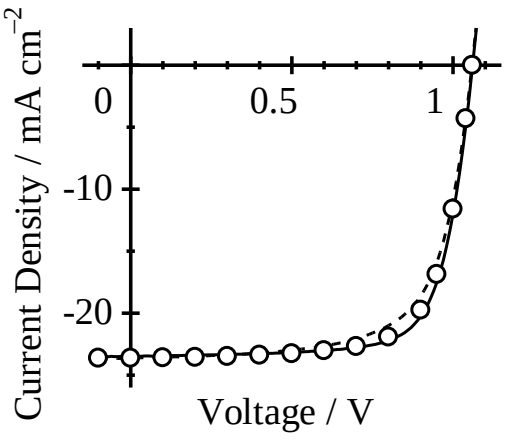

Fig. 4. J–V characteristics of a perovskite solar cell prepared from 55 wt% $CH_3NH_3PbI_3$ solution. The solid and broken lines represent J–V characteristics measured from 1.2 to −0.10 V (reverse scan) and from −0.10 to 1.2 V (forward scan) with a delay time of 1 s. The open circles represent the steady-state J–V.

hysteresis in the *J*–*V* characteristics is so small, which has no impact on J_{SC} and V_{OC}. Thus, we can safely discuss J_{SC} and V_{OC} quantitatively without considering the hysteresis. The photovoltaic parameters for the other devices employed in this study are summarized in Table 1.

Table 1. Photovoltaic parameters for $CH_3NH_3PbI_3$ perovskite solar cells with different grain sizes

Grain size / nm	J_{SC} / mA cm^{-2}	V_{OC} / V	FF	PCE / %
~100	17.0	1.00	0.590	10.0
~300	22.1	1.04	0.732	16.8
~500	23.9	1.08	0.750	19.4

Limiting factors

We first discuss the limiting factor for the J_{SC} in these perovskite solar cells with different grain sizes. As shown in Figure 5, the larger J_{SC} is due to the larger EQE at the longer wavelength region. This is simply because of the larger absorption in the thicker devices. Indeed, the internal quantum efficiency (IQE) was estimated to be ~100% for all the devices. For the thickest device, the EQE was as high as >90%, which is almost the upper limit considering the optical reflection loss.[12] Thus, these findings indicate that there is no loss in the photocurrent generation in $CH_3NH_3PbI_3$ perovskite solar cells. Note that the J_{SC} observed is in good agreement with the photocurrent calculated from the EQE and solar spectra.

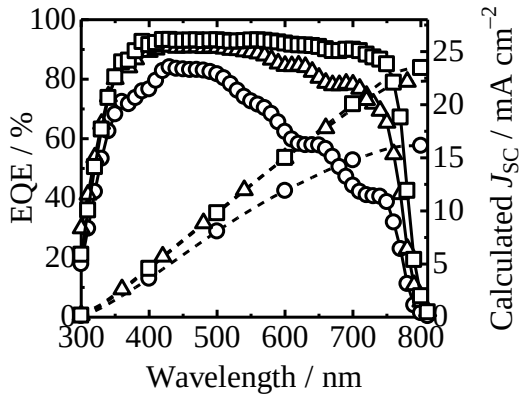

Fig. 5. EQE spectra of perovskite solar cells with different grain sizes (solid lines): ~100 nm (open circles), ~300 nm (open triangles), and ~500 nm (open squares). The broken lines represent the photocurrent density calculated from the EQE and solar spectra.

We next discuss the limiting factor for the V_{OC} in these perovskite solar cells with different grain sizes. In general, the V_{OC} is given by Eq 1

$$qV_{OC} = E_g - k_B T \ln\left(\frac{N_C N_V}{np}\right) \quad (1)$$

where q is the elementary charge, k_B is the Boltzmann constant, E_g is the optical bandgap of the active layer, N_C and N_V are the effective density of state in the conduction and valence bands, respectively, and n and p are the electron and hole density, respectively, in the active layer. On the other hand, the photocurrent generation rate G (= J_{SC}/qL) is equal to the recombination rate R in the active layer. Here, we consider the direct recombination R_{rad} and the trap-assisted Shockley–Read–Hall (SRH) recombination R_{SRH}. In other words, the overall recombination rate R is given by Eq 2

$$\begin{aligned} R &= R_{rad} + R_{SRH} \\ &= \left(B_{rad} + \frac{C_n C_p N_t}{C_n(n+n_1) + C_p(p+p_1)}\right)(np - n_i p_i) \end{aligned} \quad (2)$$

where B_{rad} is the radiative recombination coefficient, C_n and C_p are the capture coefficients for electrons and holes at trapped sites, respectively, N_t is the density of trap states, n_1 and p_1 are the density of electrons and holes, respectively, when the Fermi levels of electron and hole are equal to the trap level, and n_i and p_i are the intrinsic density of electrons and holes, respectively. As shown in Figure 6, the intensity dependence of V_{OC} can be analyzed by using Eqs 1 and 2 with different trap densities. Consequently, the trap density N_t was estimated to be 5.3×10^{16} cm^{-3} (L = ~100 nm), 1.1×10^{16} cm^{-3} (L = ~300 nm), and 2.8×10^{15} cm^{-3} (L = ~500 nm).

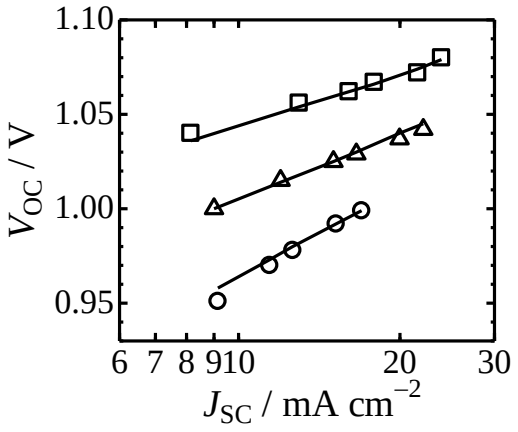

Fig. 6. Relationship between the open-circuit voltage V_{OC} and the short-circuit current density J_{SC} of $CH_3NH_3PbI_3$ perovskite solar cells with different grain sizes: ~100 nm (open circles), ~300 nm (open triangles), and ~500 nm (open squares). The solid lines represent the calculated values based on Eq 2 with trap densities: 5.3×10^{16} cm^{-3} (~100 nm), 1.1×10^{16} cm^{-3} (~300 nm), and 2.8×10^{15} cm^{-3} (~500 nm).

This finding indicates that larger grains exhibit higher quality with less trap sites.

Finally, we estimate the possible PCE of $CH_3NH_3PbI_3$ perovskite solar cells on the basis of these analyses. As mentioned above, the J_{SC} observed is as high as ~24 mA cm^{-2}, which would be almost the upper limit. The upper limit of the V_{OC} can be estimated to be 1.27 V if the N_t could be reduced to ~10^{10} cm^{-3}, which is comparable to that reported for $CH_3NH_3PbI_3$ single crystals.[13] The highest FF reported so far is as high as 0.85.[14] We therefore estimate the upper limit of the PCE to be >25%, which is comparable to that of crystalline silicon solar cells.[15]

4. Conclusions

We fabricated highly efficient perovskite solar cells with different sizes of $CH_3NH_3PbI_3$ grains by the FDC method. As a result, we found that all the photovoltaic parameters were improved with increasing grain sizes. For the solar cell with the largest grain size of ~500 nm, the highest photovoltaic parameters were obtained: J_{SC} = 23.9 mA cm^{-2}, V_{OC} = 1.08 V, FF = 0.750, and PCE = 19.4%. By analyzing the EQE and absorption spectra, we found that there is no loss in the charge generation in $CH_3NH_3PbI_3$ solar cells with a grain size of ~500 nm. This finding suggests that the J_{SC} (~24 mA cm^{-2}) observed would be almost the upper limit. By analyzing the ideality factors on the basis of the direct and SRH recombination model, we found that the larger V_{OC} obtained for the larger grains is due to the smaller trap densities in $CH_3NH_3PbI_3$ grains. We estimate the upper limit of V_{OC} to be 1.27 V on the assumption that the trap density could be reduced to ~10^{10} cm^{-3}. We therefore conclude that it would be possible to improve the PCE up to >25% if low trap density (~10^{10} cm^{-3}) and high FF (0.85) reported so far could be achieved at the same time.

Acknowledgments

This work was partly supported by the Precursory Research for Embryonic Science and Technology (PRESTO) program (Photoenergy and Conversion Systems and Materials for the Next-Generation Solar Cells) and the Advanced Low Carbon Technology Research and Development (ALCA) program (Solar Cell and Solar Energy Systems) from the Japan Science and Technology Agency (JST), and was partly based on the results obtained from a project commissioned by the New Energy and Industrial Technology Development Organization (NEDO).

References

1) W. S. Yang, J. H. Noh, N. J. Jeon, Y. C. Kim, S. Ryu, J. Seo and S. I. Seok: Science 348 (2015) 1234.

2) N.-G. Park, M. Grätzel, T. Miyasaka, K. Zhu and K. Emery: Nat. Energy 1 (2016) 16152.

3) J.-P. Correa-Baena, A. Abate, M. Saliba, W. Tress, T. J. Jacobsson, M. Grätzel and A. Hagfeldt: Energy Environ. Sci. (2017). DOI: 10.1039/C6EE03397K.

4) A. Kojima, K. Teshima, Y. Shirai and T. Miyasaka: J. Am. Chem. Soc. 131 (2009) 6050.

5) M. M. Lee, J. Teuscher, T. Miyasaka and H. J. Snaith: Science 338 (2012) 643.

6) H. J. Snaith, A. Abate, J. M. Ball, G. E. Eperon, T. Leijtens, N. K. Noel, S. D. Stranks, J. T.-W. Wang, K. Wojciechowski and W. Zhang: J. Phys. Chem. Lett. 5 (2014) 1511.

7) E. L. Unger, E. T. Hoke, C. D. Bailie, W. H. Nguyen, A. R. Bowring, T. Heumüller, M. G. Christoforo and M. D. McGehee: Energy Environ. Sci. 7 (2014) 3690.

8) N. J. Jeon, J. H. Noh, Y. C. Kim, W. S. Yang, S. Ryu and S. I. Seok: Nat. Mater. 13 (2014) 897.

9) M. Xiao, F. Huang, W. Huang, Y. Dkhissi, Y. Zhu, J. Etheridge, A. Gray-Weale, U. Bach, Y.-B. Cheng and L. Spiccia: Angew. Chem. Int. Ed. 126 (2014) 10056.

10) N. Ahn, D.-Y. Son, I.-H. Jang, S. M. Kang, M. Choi and N.-G. Park, J. Am. Chem. Soc. 137 (2015) 8696.

11) H. D. Kim, H. Ohkita, H. Benten and S. Ito: Adv. Mater. 28 (2016) 917.

12) J. M. Ball, S. D. Stranks, M. T. Hörantner, S. Hüttner, W. Zhang, E. J. W. Crossland, I. Ramirez, M. Riede, M. B. Johnston, R. H. Friend and H. J. Snaith: Energy Environ. Sci. 8 (2015) 602.

13) D. Shi, V. Adinolfi, R. Comin, M. Yuan, E. Alarousu, A. Buin, Y. Chen, S. Hoogland, A. Rothenberger, K. Katsiev, Y. Losovyj, X. Zhang, P. A. Dowben, O. F. Mohammed, E. H. Sargent and O. M. Bakr: Science 347 (2015) 519.

14) C.-G. Wu, C.-H. Chiang, Z.-L. Tseng, M. K. Nazeeruddin, A. Hagfeldt and M. Grätzel: Energy Environ. Sci. 8 (2015) 2725.

15) M. A. Green, K. Emery, Y. Hishikawa, W. Warta, E. D. Dunlop, D. H. Levi and A. W. Y. Ho-Baillie: Prog. Photovolt: Res. Appl. 25 (2017) 3.